

VISCOSITY EFFECT ON SOIL SETTLEMENTS AND PILE SKIN FRICTION DISTRIBUTION DURING PRIMARY CONSOLIDATION

Salma Al Kodsi¹, Kazuhiro Oda² and Talal Awwad³

¹Faculty of Civil Engineering, Osaka University, Japan; ² Osaka Sangyo University, Japan; ³ L.N. Gumilyov Eurasian National University, Kazakhstan

Corresponding Author, Received: 19 Jul. 2018, Revised: 06 Oct. 2018, Accepted: 25 Oct. 2018

ABSTRACT: Skin friction distribution occurs due to a relative movement between pile and adjacent soil. Varied factors affecting this movement get the soil to, occasionally, settle more than that of the pile. In this case, negative skin friction distributes along some part of the pile's shaft. Primary consolidation begins after applying surcharge load on ground surface next to pile's head - where pressure will be carried by the pore water until the entire excess pore pressure dissipates and shear stress is mobilized. This paper presents a finite element parametric study to investigate the effect of viscosity on soil settlements and skin friction distribution along the pile during primary consolidation. Single pile in clay soil is modelled using FORTRAN in conjunction with two different soil constitutive models. On the one hand, numerical modeling has been carried out using the elasto-plastic soil behavior – as defined by Matsui-Abe soil constitutive model. On the other hand, the effect of viscosity has been modeled using the elasto-viscoplastic soil model as defined by Sekiguchi-Ohta model. A parametric study has been conducted in order to compare the results of the above two soil models to clarify the viscous impact. FORTRAN 2-D analytical model has been validated by comparing numerical results with two field tests measurements. Viscosity is clearly effective when a specific value of surcharge load is applied. Structural viscosity has increased the soil settlements compared to the other settlements that occurred by using elasto-plastic soil model – where part of the pile induced by negative skin friction becomes greater.

Keywords: Negative skin friction, Finite element, Pile, Soil Model, Viscosity

1. INTRODUCTION

Applying surcharge load on the ground surface causes settlements to occur in the soil layers, and negative and positive skin friction to mobilize. Pile foundations are widely used whereas studying the behavior of clay soils is very significant and affect the pile stability.

Terzaghi [13] proposed the theory of one-dimensional consolidation of soil in 1923 describing that stress-strain behavior of cohesive, normally consolidated soils are rate-dependent. This is mainly because of the time necessity that requires the excess water pressure to dissipate. The pressure then transfers to the soil skeleton leading the settlements to continue due to structural viscosity. In their research, Toshihisa and Fusao [1] derived a three-dimensional constitutive equation of normally consolidated clay. This equation can explain the behavior of time-dependent, stress relaxation and strain rate effect. In addition, the proposed theory has a feature to be able to determine the secondary consolidation rate. Bipul, Balasingam, and Goro [5] presented a constitutive relationship for one-dimensional consolidation of clays. The importance of structural viscosity on clay consolidation has been recognized. Moreover, the viscous effect through consolidation is less at the initial stage, and likely to increase gradually along with the progress of consolidation. Tung-Lin [14]

concluded that displacement and pore water pressure of clay stratum are strongly related to the viscosity effect. The overestimation of soil displacement will occur only when the viscosity effect is being neglected. Behzad, Thu, Minh, and Hadi [4] considered the modified Cam-Clay model to simulate soil creep using finite element technique. The study showed creep index impact on increasing pore water pressure and settlement of ground under embankment. Jia-Cai Liu and Xu-Dong Wang [7] used the Voigt model to simulate various visco-elastic properties of marine clay. The used model clarified how viscosity coefficient of clay influenced the consolidation behavior. Arpan and Sujit [3] developed a 3-D consolidation apparatus and performed a series of 3-D consolidation test under different surcharge pressures. The study showed how the consolidation characteristics were largely affected by the surcharge pressure where increasing the surcharge on the surrounding soil makes it denser to reduce both the lateral movements of soil particles and the lateral pore water pressure. Determining the location of the neutral plane and negative skin friction distribution along single pile using two different soil models by carrying on a parametric study, in addition, to examine the effect of loading on the pile and clay settlements were proposed as in [2,11].

Several studies have been done to examine the distribution of skin friction along single and pile

groups. Thus, the main purpose of this paper is to study the effect of viscosity on this distribution by comparing two different soil models. The viscous effect is time-dependent and usually, its influence clearly notices during secondary consolidation. However, in this study, this influence will be studied during primary consolidation process. The value of applied surcharge load will play a rule showing viscous effect. Two field tests will be used herein to validate the soil models; and a finite element parametric study will be conducted using one of the field tests as a numerical model to cover three cases of surcharge loading.

2. FIELD TESTS

2.1 Suehiro Pile Field Test

Matsui [9] carried out a full-scale loading test of a cast-in-place RC bored pile in Osaka Bay, Osaka, Japan. The soil profile consisted of both Holocene Deposits and Upper Pleistocene Deposits. The Holocene layers consisted of loose and soft silts and clays. A sandy gravel layer was adopted as a bearing layer of the tested pile. The tested pile was a cast-in-place RC pile with 1.5m in diameter and 28.5m in length. The vertical loading test was carried out, in accordance with the Standard of the JGS [15]. Fig.1 shows the Suehiro field test soil section.

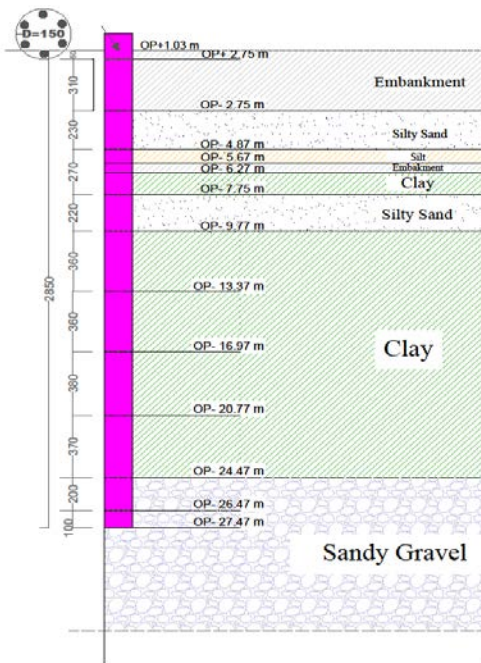


Fig.1 Soil profile of Suehiro pile field test

2.2 Ajigawa Pile Field Test

A full-scale test of a cast-in-place pile was carried out by Matsui [9] in Osaka, Japan. The soil

profile of Ajigawa pile field test consists of fine sand and silty sand layers. The main layer is a sandy silt to clay and the bearing layer is gravel. Ajigawa pile is 37.0 m in length and 2.00 m in diameter. Fig.2 shows the Ajigawa field test soil section.

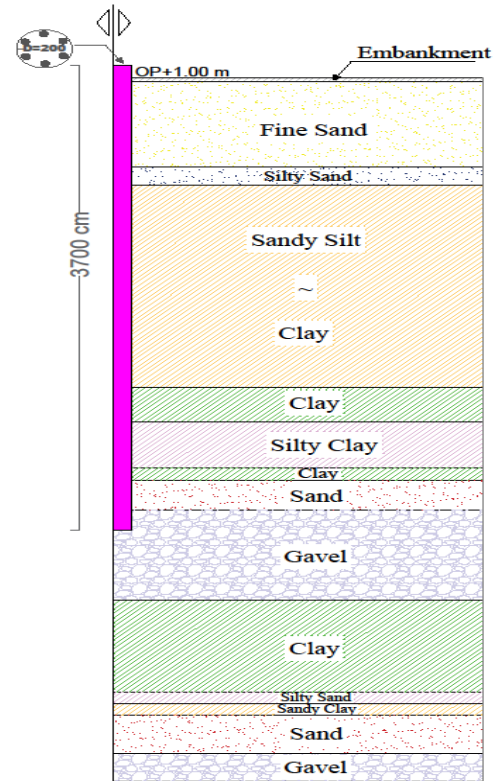


Fig.2 Soil profile of Ajigawa pile field test

3. NUMERICAL MODELING

3.1 Suehiro Pile Model Boundary, Mesh, and Initial Conditions

The model is axisymmetric in 2-D plane. The surface of the top layer of the analytical model is assumed to be permeable, while bottom and side boundaries are supposed to be impermeable. The level of groundwater is at 0.80 m down the surface. The bottom model boundary is being fixed, while the boundaries at the axis of symmetry and sides are free to move vertically. The analytical mesh was divided into 13 blocks. The first block -the pile- is divided into 360 elements acting as an elastic material. The main clay layer includes block (2) and block (3) in which both of them are divided into 234 elements. The abruption between pile shaft and surrounding soil is represented by 36 interface elements behave as jointed rock where the main clay layer includes 6 joint elements and their deformability can be described by the character of stress-deformation curves [6]. Fig.3 shows the analytical study model and mesh boundary for Suehiro pile.

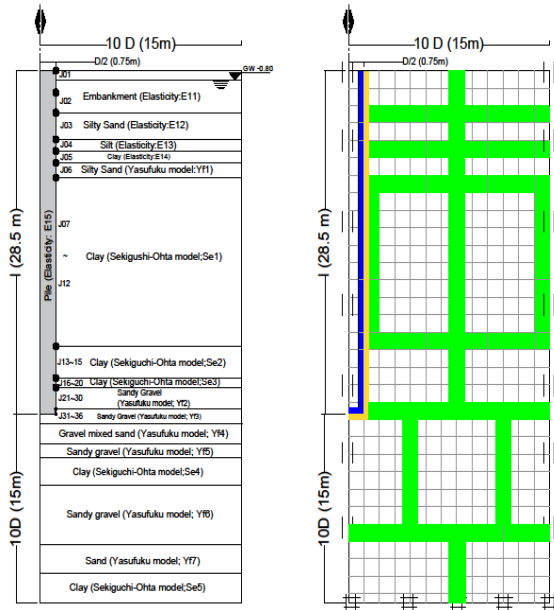


Fig.3 Suehiro pile analytical model and mesh

3.2 Ajigawa Pile Model Boundary, Mesh, and Initial Conditions

The upper layer of analytical model of Ajigawa pile is an embankment assumed to be permeable. The bottom and side boundaries are assumed to be impermeable where bottom boundary is fixed. The sides boundaries are free to move vertically. Groundwater level is at 0.70 m down the surface.

The mesh of Ajigawa pile was divided into 13 blocks. First block (pile) was divided into 360 elements as an elastic material. The main layer includes both block (2) and block (3) behave as elasto-plastic materials. Fig.4 shows the analytical study model and mesh boundary for Ajigawa pile.

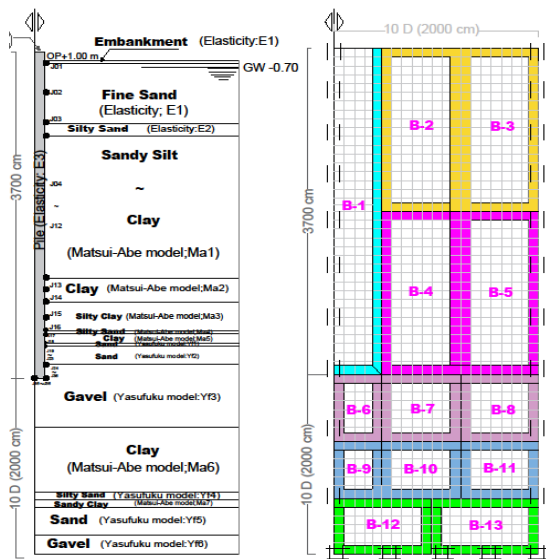


Fig.4 Ajigawa pile analytical model and mesh

3.3 Soil Constitutive Model

Two soil constitutive models will be used; an elasto-plastic soil model of Matsui and Abe [8], and an Elasto-viscoplastic soil constitutive model defined by Sekiguchi and Ohta [12] to represent the correlation between stress and strain for the main clay layer. Moreover, the bearing layer will be modeled as defined by Yasufuku soil model for sandy soils.

The elasto-plastic model is represented in Eq. (1) and Eq. (2). Yield surface (f) of Sekiguchi-Ohta and Yasufuku model are given by Eq. (3) and Eq. (4), respectively.

$$e_0 - e = \lambda \ln \left(\frac{p'}{p'_0} \right) + (\lambda - \kappa) \left(\frac{\alpha_a}{\alpha_a - 1} \right) \ln \left\{ \frac{M_a + (\alpha_a - 1)\eta}{M_a + (\alpha_p - 1)\eta_{k0}} \right\}$$

For the active state (1)

$$e_0 - e = \lambda \ln \left(\frac{p'}{p'_0} \right) + (\lambda - \kappa) \left(\frac{\alpha_p}{1 - \alpha_p} \right) \ln \left\{ \frac{M_p + (1 - \alpha_p)\eta_{k0}}{M_p + (1 - \alpha_p)\eta} \right\}$$

For the passive state (2)

Where e is the void ratio, e_0 is the initial value of e , λ is the compression index, κ is the swelling index and α_a , α_p are the strain increment ratio.

$$f = \mu \ln \left[\frac{1}{\delta} \left\{ 1 - \exp \left(- \frac{\delta v_r^v}{\mu} \right) \right\} \exp \left(\frac{v^p}{\mu} \right) + \delta \exp \left(- \frac{\delta v_r^v}{\mu} \right) \right] - v^p = 0 \quad \dots \dots (3)$$

Where μ is the coefficient of secondary consolidation, v_r^v is the reference viscous volume strain rate, δ is a material constant and v^p is the plastic volumetric strain.

$$f = \ln \frac{p}{p_0} + \frac{C}{2(C-1)} \ln \left[\frac{(1-C)(2\alpha-\eta)\eta + \{N-(2-C)\alpha\}N}{(1-C)\alpha^2 + \{N-(2-C)\alpha\}N} \right] = 0 \quad \dots \dots (4)$$

Where N and C are experimental parameters, where C has two components C_g and C_f , α is an internal parameter to reflect the influence of the proportional loading path on the yield surface and

$\eta = \frac{q}{p'}$ is the stress ratio, where q is the deviator stress and p' is the mean effective stress.

4. MODEL VALIDATION

The numerical model will be compared with the available field test measurements of Suehiro and Ajigawa piles to validate its efficiency. The elasticity parameters for pile material, analytical

parameters of Matsui-Abe, Yasufuku model parameters, Sekiguchi-Ohta parameters and the parameters of the interface elements of Suehiro pile are all shown in Table 1, Table 2, Table 3, Table 4, and Table 5, respectively. While Table 6 shows the elasticity parameters of pile materials for Ajigawa pile, Table 7, Table 8 presents the analytical parameters for Matsui-Abe and Yasufuku model, respectively. All parameters were determined through soil investigations including SPT and CPT by [10] and been used in other studies [11].

Table 1 Elasticity parameters/Suehiro pile

No.	E (kN/m ²)	ν
E11	8.40E+04	0.47
E12	2.70E+04	0.47
E13	3.00E+04	0.35
E14	1.50E+04	0.30
E15	2.20E+07	0.22

Note: E is the Elastic modulus, ν is the Poisson ratio

Table 2 Matsui-Abe model parameters/Suehiro pile

No.	λ	κ	M
Ma1	0.2480	0.0124	1.41
Ma2	0.4950	0.0248	1.26
Ma3	0.4000	0.0248	1.26
Ma4	0.5800	0.0243	1.26
Ma5	0.4480	0.0224	1.32

Note: λ is the slope of normally consolidation line. κ is the slope of the elastic swelling line. M is the frictional constant. Poisson ratio (ν) =0.33

Table 3 Sekiguchi-Ohta model parameters/Suehiro pile

No.	λ	κ	M
Se1	0.1024	0.01240	1.47
Se2	0.2475	0.01240	1.41
Se3	0.2475	0.01240	1.41
Se4	0.4950	0.02480	1.41
Se5	0.5800	0.02430	1.26

Table 4 Yasufuku model parameters/Suehiro pile

No.	N	M
Yf1	1.90E-02	0.75
Yf2	2.82E-03	0.80
Yf3	2.82E-03	0.75
Yf4	2.82E-03	0.75
Yf5	3.27E-03	0.80
Yf6	2.82E-03	0.8
Yf7	3.27E-03	0.75

Note: α , C are constant. $\alpha = 0.4$, $C_g = 2.0$, $C_f = 1.5$

Table 5 Interface elements parameters/Suehiro pile

No.	Kn (kN/m ³)	Ks (kN/m ³)	C0(kN/m ²)
J01	9.8×10 ⁹	9.8×10 ⁹	15.55
J02	9.8×10 ⁹	9.8×10 ⁹	11.86
J03	9.8×10 ⁹	9.8×10 ⁹	19.58
J04	9.8×10 ⁹	9.8×10 ⁹	8.33
J05	9.8×10 ⁹	9.8×10 ⁹	9.07
J06	9.8×10 ⁹	9.8×10 ⁹	8.28
J07	9.8E+09	9.8E+09	5.64
J08	9.8E+09	9.8E+09	17.29
J09	9.8E+09	9.8E+09	15.90
J10	9.8E+09	9.8E+09	11.52
J11	9.8E+09	9.8E+09	15.01
J12	9.8E+09	9.8E+09	10.97
J13	9.8×10 ⁹	9.8×10 ⁹	10.40
J14	9.8×10 ⁹	9.8×10 ⁹	13.23
J15	9.8×10 ⁹	9.8×10 ⁹	12.87
J16	9.8×10 ⁹	9.8×10 ⁹	13.29
J17	9.8×10 ⁹	9.8×10 ⁹	9.09
J18	9.8×10 ⁹	9.8×10 ⁹	9.41
J19	9.8×10 ⁹	9.8×10 ⁹	5.89
J20	9.8×10 ⁹	9.8×10 ⁹	11.53
J21	9.8×10 ⁹	9.8×10 ⁹	34.56
J22	9.8×10 ⁹	9.8×10 ⁹	28.65
J23	9.8×10 ⁹	9.8×10 ⁹	43.03

J24	9.8×109	9.8×109	42.14
J25	9.8×109	9.8×109	36.43
J26	9.8×109	9.8×109	28.85
J27	9.8×109	9.8×109	33.26
J28	9.8×109	9.8×109	38.46
J29	9.8×109	9.8×109	32.61
J30	9.8×109	9.8×109	34.37
J31	9.8×109	9.8×109	37.00
J32	9.8×109	9.8×109	28.52
J33	9.8×109	9.8×109	42.45
J34	9.8×109	9.8×109	39.23
J35	9.8×109	9.8×109	37.01
J36	9.8×109	9.8×109	25.99

Note: Kn, Ks is the slope of the elastic line in compression state and shear deformation state, respectively, C0 is cohesion factor between the pile shaft and surrounding soil. θ is the internal angle of friction = 0

Table 6 Elasticity parameters/Ajigawa pile

No.	E (kN/m ²)	ν
E1	8.40E+01	0.20
E2	5.60E+01	0.20
E3	3.10E+05	0.22

Table 7 Matsui-Abe model parameters/Ajigawa pile

No.	λ	κ	M
Ma1	0.6713	0.0671	1.20
Ma2	0.0530	0.0053	1.20
Ma3	1.0017	0.1002	1.20
Ma4	0.5360	0.0536	1.20
Ma5	0.5500	0.0500	1.20
Ma6	0.3650	0.0365	1.20
Ma7	0.2069	0.0207	1.20

Table 8 Yasufuku model parameters/Ajigawa pile

No.	N	M
Yf1	1.90E-02	0.75

Yf2	2.82E-03	0.80
Yf3	2.82E-03	0.75
Yf4	2.82E-03	0.75
Yf5	3.27E-03	0.80
Yf6	2.82E-03	0.8
Yf7	3.27E-03	0.75

Modeling using Suehiro pile data, the comparison between numerical results and field test measurements to determine the pile axial load distribution in case of elasticity and viscosity is shown in Fig. 5. In addition, a comparison between pile's head and toe displacement is also shown in Fig. 6 and Fig. 7. With regard to Ajigawa pile, the comparison is done for the case of elastic-plastic only as shown in Fig. 8, Fig.9 and Fig. 10.

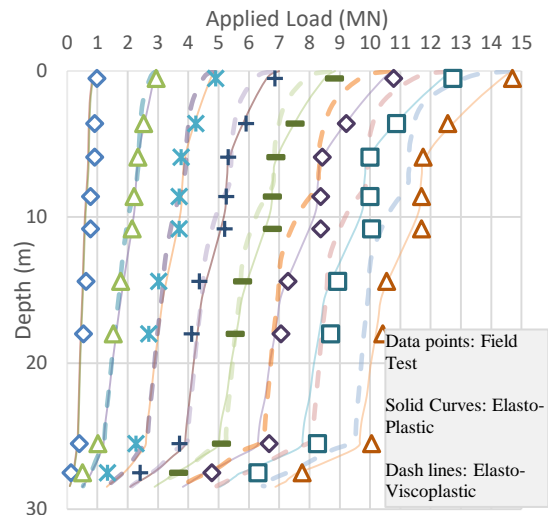


Fig.5 Pile axial load distribution/Suehiro pile

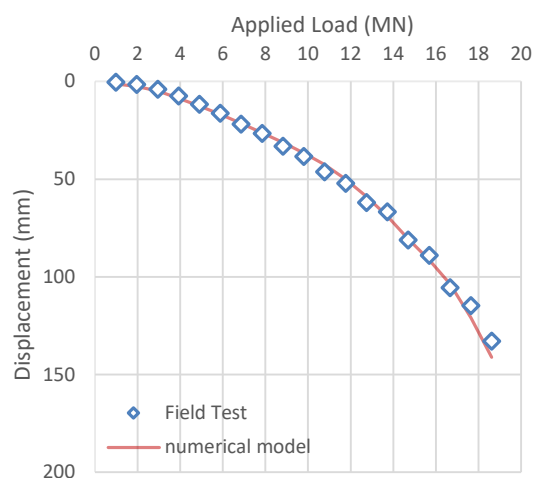


Fig.6 Pile head displacement/ Suehiro pile

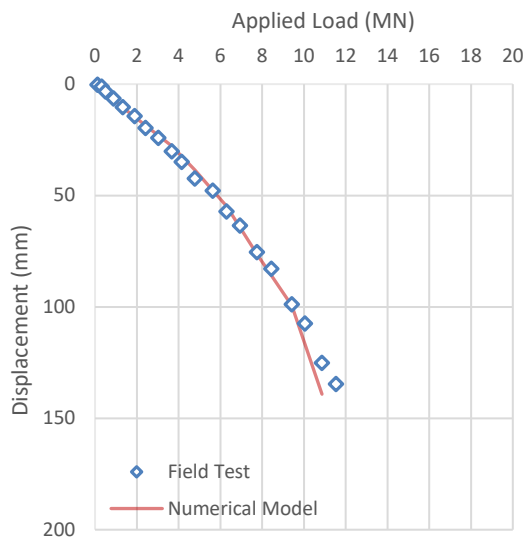


Fig.7 Pile toe displacement/ Suehiro pile

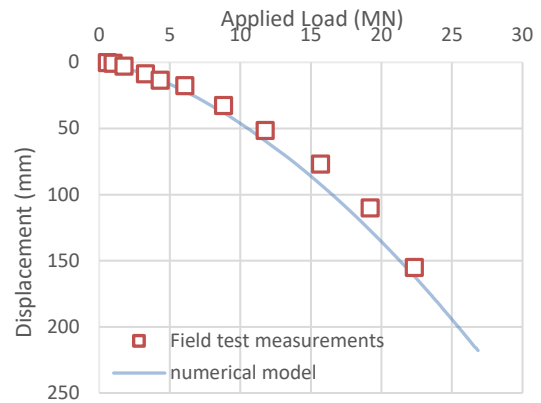


Fig.10 Pile toe displacement/ Ajigawa pile

Depending on the comparison results, the numerical model is valid and can be used to carry on the parametric study.

6. PARAMETRIC STUDY

In the parametric study, three cases of pile and surcharge load have been used to determine soil settlements and negative skin friction distribution along Suehiro pile as shown in Table 9.

Table 9 Parametric study cases

Case	PL*	SL**
1	100	2.0
2	100	4.0
4	100	8.0

*Pile load (tf), ** Surcharge load (tf/m²)

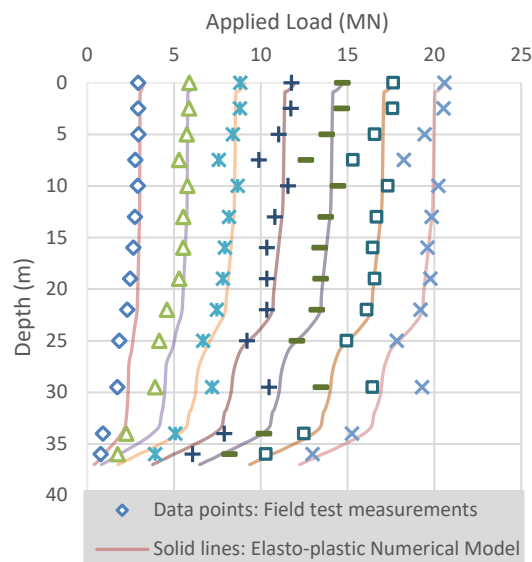


Fig.8 Pile axial load distribution/ Ajigawa pile

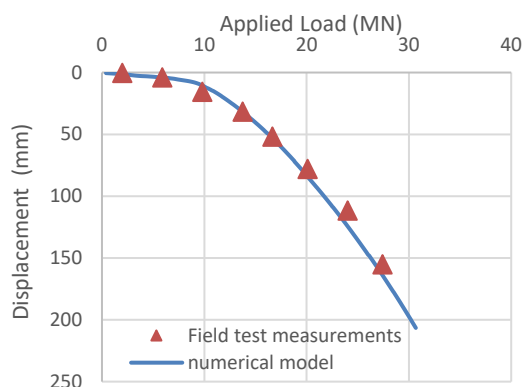


Fig.9 Pile head displacement/ Ajigawa pile

When 2.0 tf/m² of surcharge load was applied on the ground surface, a noticeable difference in settlements occurred between the two soil models. The ground displacements were larger in case of modeling using elastic-viscoplastic soil model. It can be noticed that viscosity had an influence during primary consolidation similar to elastic-plastic at the beginning of consolidation process. And with time, this influence start to be larger, especially at the middle of primary consolidation down to the end where elastic-plastic settlements stopped and the other continued to occur entering secondary consolidation stage as shown in Fig. 11.

In case of applying a higher value of surcharge pressure – 8.0 tf/m²-, the situation was different. Settlements for the two used soil models were almost similar at the beginning of consolidation until the end, where the difference start to be noticed as the secondary consolidation process starts.

As the skin friction distribution is related to soil settlements, no difference in skin friction distribution occurred between the two soil models when a large surcharge load was applied, Fig. 12.

In case of applying a small surcharge load, structural viscosity had an impact on negative skin friction distribution comparing to elasticity. The part of pile was induced by negative skin friction using elasto-viscoplastic model were about 10 m more. Fig. 13 and Fig. 14 are shown the different in the location of neutral plane which is the line separates negative friction from positive.

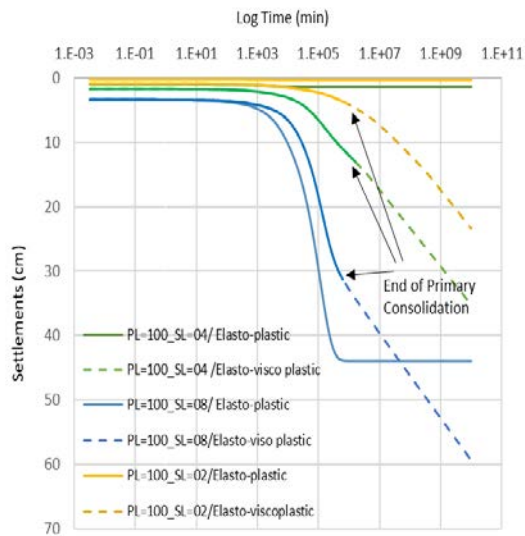


Fig. 11 Comparison between Elasto-plastic and Elasto-viscoplastic model – Soil ground settlements with time

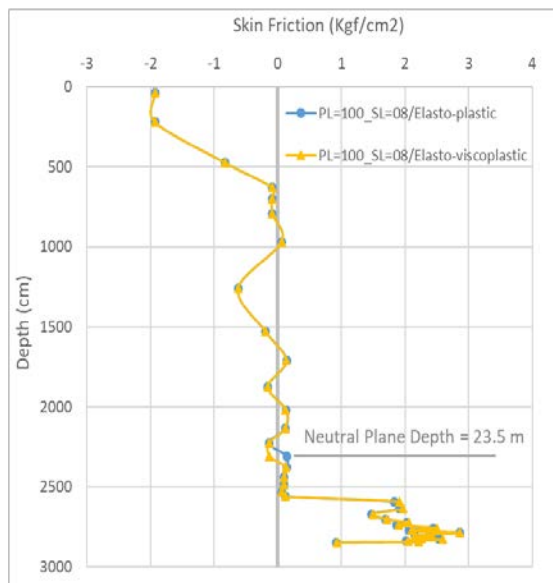


Fig. 12 A comparison between Elasto-plastic and Elasto-viscoplastic model – Skin friction distribution

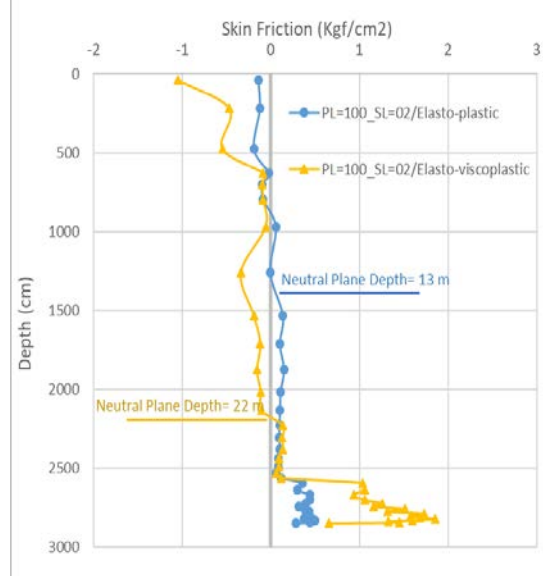


Fig. 13 A comparison between Elasto-plastic and Elasto-viscoplastic model – Skin friction distribution.

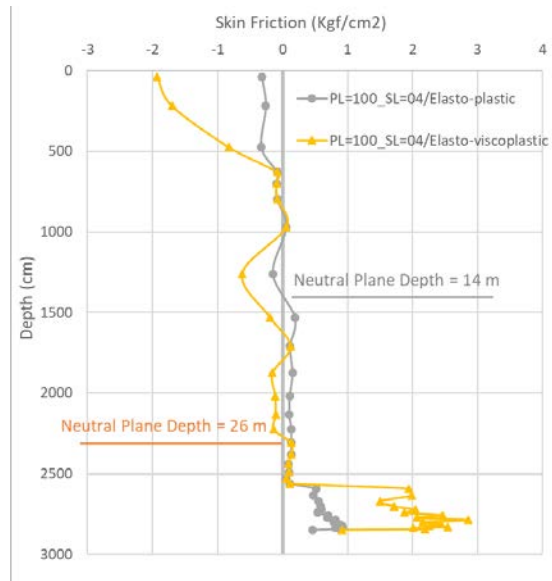


Fig. 14 Comparison between Elasto-plastic and Elasto-viscoplastic model – Skin friction distribution

7. CONCLUSION

Applying a surcharge load on the ground surface played the main role in mobilizing skin friction along the pile's shaft due to clay layers' settlements. This paper was aimed to examine the effect of viscosity on changing the soil settlement and the skin friction distribution. The soil settlements, skin friction distribution and neutral plane location were

determined using two different soil constitutive models.

It can be noticed that when elasto-viscoplastic soil model was used, the soil settlements and the skin friction distribution have been increased even though the study has been done during the primary consolidation stage. This effect has been noticed clearly in case of small values of surcharge load. However, when the surcharge load exceeded a specific amount, viscous influence was approximately similar to elasto-plastic. Applying large value of surcharge load caused the soil to settle equally in both models especially at the beginning of the primary consolidation until the middle of the process.

The location of the neutral plane was influenced by the viscous effect. As the settlements and negative skin friction increased due viscosity, the part of the pile induced by negative skin friction was greater and the neutral plane location went deeper.

Moreover, in the case of modeling using elasto-viscoplastic soil model, the primary consolidation process finished in a shorter time than in the case of elasto-plastic. As the viscosity had an impact on soil settlements, it is recommended to model using elasto-viscoplastic soil model especially if the ground surface will be loaded with a small value of surcharge load for a long term. According to all mentioned above, it is important to take the viscous effect into consideration when designing pile foundations and carrying on this study to examine the soil behavior and skin friction distribution during secondary consolidation due to structural viscosity.

8. REFERENCES

- [1] Adachi, T. and Oka, F. (1982). Constitutive equations for normally consolidated clay based on elasto-viscoplasticity. *Soils and foundations*, 22 (4), 57-70.
- [2] Awwad, T. and Kodsí, S.A. (2017). A comparison of numerical simulation models to determine the location of the neutral plane. *Proceedings of the 19th International Conference on Soil Mechanics and Geotechnical Engineering*. pp 1947 – 1950.
- [3] Arpan, L. and Sujit, K. P. (2017). The effect of different surcharge pressure on 3-D consolidation of soil. *International journal of applied engineering research* ISSN 0973-4562 Volume 12, number 8 (2017), pp. 1610-1615.
- [4] Behzad, F., Thu, M.L., Minh, L., Hadi, K., (2013). Soil creep effects on ground lateral deformation and pore water pressure under embankments. *Geomechanics and Geoen지니어ing*. June 2013.
- [5] Bipul, C. H., Balasingam, M., Goro, I. (2003). Viscosity effects on one-dimensional consolidation of clay. *International Journal of Geomechanics*, Vol. 3, No. 1, September 1, 2003.
- [6] Goodman, R.E., Taylor, R.L., & Brekke, T.L. (1968). A Model for the Mechanics of Jointed Rock. *Journal of the Soil Mechanics and Foundations Division, ASCE* 94, SM3, pp.637-659.
- [7] Jia-cai, L. and G. H. Lei, Xu. (2015). One-dimensional consolidation of visco-elastic marine clay under depth-varying and time-dependent load. *Marine Georesources and Geotechnology* 33(4), July 2015.
- [8] Matsui, T. and Abe, N. (1981). Multi-dimensional elasto-plastic consolidation analysis by finite element method. *Soils and Foundations*, vol. 21, No. 1, pp. 79-95.
- [9] Matsui, T. (1993). Case studies on cast-in-place bored piles and some considerations for design, *Deep Foundations on Bored and Auger Piles*. Ghent, pp. 77-101
- [10] Oda, K. (2012). Numerical simulations of field loading tests of cast-in-place bored piles with a large diameter. *Testing and Design Methods for Deep Foundations*, pp.859-866, 2012.09, *International Conference(Proceedings)*
- [11] Kodsí S.A., Oda K. (2019) Numerical Simulation and Parametric Study of a Single Pile in Clay Layer to Examine the Effect of Loading on Settlements and Skin Friction Distribution. In: Khabbaz H., Youn H., Bouassida M. (eds) *New Prospects in Geotechnical Engineering Aspects of Civil Infrastructures*. GeoChina 2018. Sustainable Civil Infrastructures. Springer, Cham
- [12] Sekiguchi, H. and Ohta, H. (1977). Induced anisotropy and time dependency in clays. 9th ICSMFE, Tokyo, *Constitutive equations of Soils*, pp.229-238.
- [13] Terzaghi, K., (1941). Undisturbed clay samples and undisturbed clays. *Journal of Boston Society of Civil Engineering*, 29 (3), 211-231.
- [14] Tung-Lin, T. (2009). Viscosity effect on consolidation of poroelastic soil due to groundwater table depression. *Environ Geol* (2009) 57:1055–1064.
- [15] Japanese Geotechnical Society (1972) Standard method for vertical loading tests of piles (in Japanese).